JOURNAL OF GEOPHYSICAL RESEARCH, VOL. 104, NO. D4, PAGES 3993-4003, FEBRUARY 27, 1999

In situ measurements of effective diameter and effective droplet number concentration

Alexei V. Korolev, George A. Isaac, and J. Walter Strapp
Atmospheric Environment Service, Downsview, Ontario, Canada

Anatoly N. Nevzorov
Central Aerological Observatory, Moscow, Russia

Abstract. The effective diameter of cloud droplets is usually derived from measurements of droplet size distribution measured by Particle Measuring Systems (PMS) probes. The disadvantage of this method is that PMS probes have a truncated size range. During the RACE project, an alternative method to measure the effective diameter used a cloud extinction meter and King and Nevzorov hot wire liquid water content and total water content (LWC/TWC) probes installed on the National Research Council (NRC) Twin Otter. The effective diameter was derived from direct *in situ* measurements of the extinction coefficient (ε) and liquid water content (W) as $D_{eff}=k_1 W/\varepsilon$. This method of calculation of D_{eff} is free of problems related to deriving D_{eff} from the truncated particle size distribution. Since measurements of ε and W cover the whole size range of cloud particles, this method gives an accurate value of D_{eff}. This method can also be successfully applied for mixed and ice phase clouds, since the Nevzorov TWC probe provides measurements of total (ice plus liquid) water content. Effective number concentration was calculated as $N_{eff}= k_2\varepsilon^3/W^2$. Comparisons of D_{eff} and N_{eff}, calculated by this method, and directly from PMS Forward Scattering Spectrometer Probe (FSSP) spectra, are favorable in the subset of conditions when the FSSP is considered to measure the spectra fully and accurately.

1. Introduction

Clouds have an important impact on the Earth's energy budget [*Stephens and Webster*, 1984]. The radiative properties of clouds are defined by the cloud particle size distribution as well as their shapes and orientation. By changing the droplet size distribution on a global scale, the optical properties of clouds may be altered sufficiently to change the global energy budget and hence the climate [*Twomey*, 1977; *Charlson et al.*, 1987]. Therefore it is important to adequately simulate the radiative properties of clouds in numerical weather and climate models [e.g., *Mitchel et al.*, 1989]. However, such numerical models have grid lengths which are too large to resolve explicitly the microphysical processes in clouds. Therefore a number of bulk model variables have to be parameterized to improve the model prediction. One of the most important parameters is the effective diameter of cloud particles [*Stephens*, 1978; *Slingo and Schencker*, 1982].

The effective diameter is defined as the ratio of the third and second moments, of the droplet size distribution $f(D)$ [*Hansen and Travis*, 1974)]; that is,

$$D_{eff} = \frac{\int_0^\infty f(D)D^3 dD}{\int_0^\infty f(D)D^2 dD} = \frac{\overline{D^3}}{\overline{D^2}} \quad (1)$$

where $\overline{D^2}$ and $\overline{D^3}$ are the mean square and the mean cube diameters of a droplet size distribution, respectively.

Slingo [1990] examined the sensitivity of the current climate to small variations in the bulk and microphysical properties of liquid low-level clouds. He found that decreasing the effective radius from 10 to 8 μm increases the short-wave albedo enough to offset global warming caused by CO_2 doubling. This means that accurate measurements of the cloud microphysical parameters are essential, especially in the context of parameterization of D_{eff} for climate models, which are highly sensitive to this parameter [e.g., *Dadlin et al.*, 1997].

The effective diameter is usually derived from measurements of the droplet size distribution, and the majority of research groups use PMS Forward Scattering Spectrometer Probes (FSSP) and Optical Array Probes (OAP) [*Knollenberg*, 1981] for these measurements. Though the accuracy of PMS probes has improved during the last two decades by introducing corrections [e.g., *Baumgardner and Spowart*, 1990; *Wendish et al.*, 1996; *Baumgardner and Korolev*, 1997], the calculation of D_{eff} from FSSPs and OAPs in many cases may be highly inaccurate. The disadvantage of

Paper number 1998JD200071.
0148-0227/99/1998JD200071$09.00

this method is that PMS probes have a limited size range, which truncate the actual size distribution. Droplets outside of this range may affect the calculated value of the effective diameter. For example, for nonprecipitating liquid clouds the effective diameter is frequently calculated from the measurements of only one FSSP as

$$D^{*}_{eff} = \frac{\sum_{i=1}^{15} n_i D_i^3}{\sum_{i=1}^{15} n_i D_i^2} \qquad (2)$$

where n_i is a droplet number concentration in the i th size bin centered at the droplet size D_i. The droplet size spectra can be measured by an FSSP in one of the following typical size ranges: 0.5-8 μm, 1-16 μm, 2-32 μm, 3-47 μm, and 5-95 μm. In many cases, none of these ranges can fully cover the variations of droplet size spectra caused by the natural inhomogeneity in cloud microstructure.

Several other problems arise due to idiosyncrasies and shortcomings of the instruments. One potential problem may be changes of size bin thresholds due to dirty optics and/or misalignment of the probe optics, leading to incorrect sizing of cloud droplets. In the case of a broad particle size distribution, the measured droplet size spectrum can be obtained by combining measurements from several PMS probes with truncated size ranges, which introduces the well-known problem of disagreement in the overlap regions of different PMS probes.

The particle size calculated from PMS OAP two-dimensional (2D) images in many cases is simply not accurate without relatively complex corrections for measurement errors caused by probe digitization, response time, and out of focus images [*Korolev et al.*, 1998a].

The situation is worse in the case of mixed and ice clouds. The use of an FSSP in ice and mixed clouds may give inadequate measurements. Though *Gayet et al.* [1996] showed some promising results of FSSP measurements in the case of quasi-spherical ice particles in contrail clouds, the use of the FSSP in clouds containing nonspherical ice crystals may give highly unreliable results [*Gardiner and Hallet*, 1985; *Gayet et al.*, 1996].

The effective diameter defined by equation (1) is somewhat ambiguous in the case of ice particles since it is not really clear what constitutes the "diameter" of a nonspherical particle. Currently, there is no unified approach to the definition of the effective diameter for nonspherical particles. Different authors use different definitions of the effective diameter of an ensemble of ice particles. Thus *Foot* [1988], for the calculation of the optical properties of cirrus clouds, defined the effective diameter based on PMS OAP-2DC measurements of shadow area and estimates of ice water content (IWC) as

$$D_{eff} = 2\sum_{j=1}^{N} n_j \left(0.5 D_j\right)^3 \Big/ \sum_{j=1}^{N} n_j S_j / \pi \qquad (3)$$

where n_j is summed over all particles; D_j is an equivalent diameter of sphere of density 1.0 g cm^{-3}, and S_j is the cross-sectional area of the ice particle. *Platt and Harshvardhan* [1988] consider ice particles as cylinders in their calculations of radiative transfer in cirrus clouds. They defined the effective diameter as

$$D_{eff} = 2\int_0^{\infty} n(r) r^2 L \; dL \Big/ \int_0^{\infty} n(r) r L \; dL \qquad (4)$$

where L is the length of the cylinder, r is a cylinder radius, and $n(r)$ is the distribution of ice cylinders by radii. It was assumed that r and L are related as r–$0.0285L^{0.786}$ [*Heymsfielad and Platt*, 1984]. *Ebert and Curry* [1992], for the parameterization of the optical properties of ice clouds for climate models, assumed ice particles as hexagonal cylinders. They calculated the effective diameter as

$$D_{eff} = 2\int_0^{\infty} \left(\frac{A}{4\pi}\right)^{3/2} n(L) dL \Big/ \int_0^{\infty} \frac{A}{4\pi} n(L) dL \qquad (5)$$

where A is the surface area of the particle; L is the thickness of the hexagonal cylinders, and $n(L)$ is distribution of ice cylinders by length.

It is seen that all three definitions of the effective diameter for ice particles are different. It is easy to see that for cylindrical particles the above three definitions give different results. For example, the difference between the second (equation (4)) and third (equation (5)) definitions may be a factor of 2 or even more if the ratio L/r exceeds 7. Moreover, since the first definition (equation (3)) includes the particle projection S_j, it turns out to be dependent on ice particle orientation. However, the second and third definition (equations (4) and (5)) ignore the orientation of ice particles.

In this paper, an alternative method of measuring the effective diameter is considered. This method derives the effective diameter from direct measurements of liquid water (W) and extinction coefficient (ε). The essence of this method is described in section 2. Another microphysical parameter, which can be derived from W and ε measurements, the effective concentration N_{eff}, is also introduced in section 2. This parameter is expected to be important for use in climate and Global Circulation Models (GCM). The aircraft instrumentation used for measurements of W and ε is discussed in section 3. Section 4 briefly considers the comparisons of D_{eff} and N_{eff} derived from FSSP measurements with those calculated using the proposed method.

2. Calculation of Effective Diameter and Effective Concentration

The calculations of D_{eff} and N_{eff} from direct measurements of water content and extinction coefficient are based on the following approach:

2.1. Effective Diameter

Since the liquid water content is proportional to the third moment of the droplet size distribution, that is,

$$W = \frac{\pi \rho_w}{6} \int_0^{\infty} f(D) D^3 dD \qquad (6)$$

and the extinction coefficient is proportional to the second moment of the droplet size spectrum

$$\varepsilon = \frac{k\pi}{4} \int_0^{\infty} f(D) D^2 dD \,, \qquad (7)$$

the effective diameter can be expressed through W and ε using equations (1), (6) and (7) as

$$D_{eff} = \frac{3}{\rho_w}\frac{W}{\varepsilon} \tag{8}$$

where ρ_w is the liquid water density and k is the extinction efficiency. The extinction efficiency is an oscillating function of the parameter $\alpha=\pi D/\lambda$ approaching asymptotically to 2 with an increase of α [e.g., *van de Hulst*, 1957], where λ is the wavelength of the radiation. For visible light, the oscillations can be neglected for droplets with $D>4$ μm. The effect of oscillations is also reduced for polychromatic light, since the oscillation will be averaged for the different wavelengths. In this work the extinction efficiency was approximated as $k=2$. For typical cloud droplet size distributions with a modal diameter larger than 4 μm, approximation of the extinction efficiency by 2 may cause an error in the extinction coefficient of less than 10%. However, in the vicinity of cloud base, where the extinction coefficient is mainly defined by small droplets, this approximation should be used with caution, since it may give larger errors.

The above method of calculation of effective diameter (equation (8)) was originally introduced by *Nevzorov and Shugaev* [1972] and was used for the calculation of the characteristic size of cloud particles size distributions. (In the study of *Nevzorov and Shugaev* [1972] the effective diameter was called D_{23}, since it was derived from second and third moments of the droplet size distribution, i.e., extinction and water content, respectively.) *King and Handsworth* [1979] used the ratio W/ε for estimation of the average droplet radius and droplet number concentration in liquid clouds. *Mazin et al*, [1996] applied the considered technique for the calculation of D_{eff} in clouds of different type.

2.2. Effective Concentration

Let us consider a *monodisperse* droplet size distribution with the droplet number concentration N_{eff}, droplet size D_{eff}, with the same LWC (W), extinction coefficient (ε), and effective diameter (D_{eff}) as the droplet size spectrum $f(D)$. These conditions yield the following equations:

$$W = \frac{\pi\rho_w}{6} N_{eff} D_{eff}^3 = \frac{\pi\rho_w}{6}\int_0^\infty f(D)D^3 dD \tag{9}$$

$$\varepsilon = \frac{k\pi}{4} N_{eff} D_{eff}^2 = \frac{k\pi}{4}\int_0^\infty f(D)D^2 dD \tag{10}$$

We shall define the number concentration of such a monodisperse spectrum as the effective concentration. The value of N_{eff} can be derived from equations (9) and (10) as

$$N_{eff} = \frac{2\rho_w^2}{9\pi}\frac{\varepsilon^3}{W^2} \tag{11}$$

Equations (9) and (10) yield another calculation of the effective concentration

$$N_{eff} = \frac{\left(\int_0^\infty f(D)D^2 dD\right)^3}{\left(\int_0^\infty f(D)D^3 dD\right)^2} = N_0\frac{\left(\overline{D^2}\right)^3}{\left(\overline{D^3}\right)^2} = N_0\frac{\overline{D^3}}{D_{eff}^3} = N_0\frac{\overline{D^2}}{D_{eff}^2} \tag{12}$$

where $N_0 = \int_0^\infty f(D)dD$ is the actual number concentration of droplet size distribution $f(D)$.

Equation (12) is a convenient calculation to apply to data sets such as those provided by the FSSP. Equation (12) indicates that the difference between N_0 and N_{eff} will be smaller when the difference between $\sqrt[2]{\overline{D^2}}$ and $\sqrt[3]{\overline{D^3}}$ decreases. Since for any droplet size distribution $D_{eff} \ge \sqrt[3]{\overline{D^3}} \ge \sqrt[2]{\overline{D^2}}$, then $N_0 \ge N_{eff}$ for all conditions. The effective concentration is equal to the actual droplet number concentration only for a monodisperse spectrum. The importance of N_{eff} for parameterization in climate and weather models is discussed in section 5.

2.3. Accuracy of Two Methods

This section gives a brief discussion of the accuracy of D_{eff}, N_{eff} measurements derived from the FSSP and hot wire probes, and the extinction meter data. Since the resulting accuracy depends on how each particular probe was adjusted and calibrated, the following discussion of the accuracy should be considered as general.

The accuracy of measurements of effective diameter derived from the FSSP depends on the accuracy of measurements of droplet size, and it is independent of the accuracy of the droplet number concentration. It should be noted that the measurement error also depends on the shape of the droplet size distribution and the accuracy of the droplet size of each size bin. For simple cases, when the relative measurement error is constant for each size bin, the accuracy of D_{eff} is independent of the droplet size spectrum and is equal to the accuracy of the droplet size measurements. For example, if the size of droplets is measured with a 10% accuracy for all size bins, then D_{eff} would be measured with same accuracy. The accuracy of the effective concentration measurements is linearly related with the accuracy of the total concentration measurements and, in a complex way, depends on the accuracy of measurements of droplet size in each size bin and the droplet size distribution. For the case where the relative error in size measurements is constant for all size bins, then the accuracy in the measurements of N_{eff} is independent of the shape of the droplet size spectrum and is equal to the error in the measurement of total concentration only.

For the suggested method of calculating D_{eff} from equation (8) the resulting relative accuracy of D_{eff} is equal to $(1\pm\delta_W)/(1\pm\delta_\varepsilon)$, where δ_W and δ_ε are the relative error in measurements of W and ε, respectively. For a 10% error in measurement of δ_W and δ_ε the resulting error will range from 0 to 22%, depending on the sign of the errors. The accuracy in measurements of N_{eff} can be estimated as $(1\pm3\delta_W)/(1\pm2\delta_\varepsilon)$. For a 10% error in the measurement of δ_W and δ_ε the resulting error in N_{eff} may range from 8 to 62%, depending on the sign of the errors.

The suggested method strongly depends on the accuracy of both the hot wire and the extinction probes. However, this method has an advantage in mixed and ice clouds where the accuracy stays to a first approximation the same as in liquid

clouds. The calculation of D_{eff} from PMS FSSP and OAP measurements may be highly unreliable in such clouds, as discussed in section 1.

3. Instrumentation

As shown above, the effective diameter and effective concentration can be derived from measurements of water content and extinction coefficient. The extinction coefficient and the cloud water content were measured by a cloud extinction meter and hot wire probes, respectively, and the results were compared with FSSP measurements described below.

The data were collected during the Radiation, Aerosol, and Cloud Experiment (RACE) conducted by the Atmospheric Environment Service (AES) in Nova Scotia during August-September 1995. The National Research Council (NRC) Twin Otter was equipped by the Cloud Physics Research Division (AES) with a set of instruments to measure different cloud microphysical parameters. The measurements were made in low-level, liquid, nonprecipitating marine *St-Sc*.

Droplet size spectra were measured by a PMS FSSP operated in the manufacturer's nominal 3-47 μm size range. Three corrections have been applied to the droplet size spectra. First, this FSSP is one of the original FSSPs with a single set of pulse height analyzer voltage thresholds. The authors have found that the bin diameters provided by the manufacturer contained a simple error and did not conform to the Mie-scattering curve, especially on FSSP range 0. Reassessment of the bin thresholds has been performed, resulting in a modified size range for the FSSP range 0 of 2.3-61 μm. The second correction is due to the improper primary size calibration of the probe using glass beads. Calibrations performed prior to the flights discussed in this article revealed that the probe was oversizing. It was concluded that the oversizing was due to a calibration gain resistor error and that all signals received by the probe were approximately a factor of 1.33 too high. The probe calibration gain resistor was not changed, but instead, a simple correction method was developed to redefine the bins of the FSSP, assuming a constant scattered intensity scale factor error. The redefinition resulted in a final size range for range 0 of 2.0-52.2 μm. The final correction, applied to the FSSP droplet spectra, is an enhancement of concentrations for dead time and coincidence errors [*Baumgardner et al.*, 1985; *Brenguier*, 1989]. The algorithm used for this study is that described by *Baumgardner et al.* [1985]. Because of the relatively low droplet concentrations, this correction factor was usually lower than 20%.

Liquid water content was measured by two different hot wire probes: a PMS King probe [*King et al.*, 1978] and a Nevzorov Liquid and Total Water Content (LWC/TWC) probe [*Nevzorov*, 1980; *Korolev et al.*, 1998b]. The principle of operation of the Nevzorov LWC/TWC probe is similar in many features to the PMS King probe. Both of its sensor wires operate at constant temperature, like the PMS King probe. The geometry and size of the LWC sensor wires is very similar to that of the King probe. One of the distinctive features of the Nevzorov sensors is that the convective heat transfer term is automatically compensated to a degree with the help of additional reference sensors. Both the King probe [*Biter et al.*, 1987] and the similar Nevzorov LWC probe have a diminished response with increasing droplet mean volume diameter. The TWC sensor of the Nevzorov probe has a concave conical shape that acts as a trap for cloud particle, both liquid and ice. As a consequence, not only is the response to high mean volume diameter drop spectra enhanced relative to the PMS King and Nevzorov LWC probes but also the TWC sensor measures the total liquid plus ice mass. The principle of operation of the Nevzorov LWC/TWC probe, accuracy of measurements, and illustrations of some of the properties described above are considered in more detail by *Korolev et al.* [1998b].

Measurements of the extinction coefficient were made with an airborne extinction meter [*Nevzorov and Shugaev*, 1974; *Kosarev et al.*, 1976], similar to one used on the Central Aerological Observatory research aircraft through the 1970s and 1980s. The principle of operation of this transmissometer is based on the reduction of the light intensity between an emitter and a receiver due to cloud. An incandescent tube lamp with a brightness temperature of about 3000°C is used as the source of light. A collimated light beam with 0.5° divergence is directed to a cone-cube prism and reflected backward to the optical unit, where the receiving photodiode measures the intensity of the transmitted light. The measured intensity is normalized by the intensity of the light source, and the background intensity of daylight is filtered out.

The optical unit of the extinction meter was installed on the ceiling of the Twin Otter fuselage. The reflecting cone-cube prism was mounted inside a special housing on the top of the aircraft tail (Figure 1). The distance between the optical unit and the reflecting prism was L=6 m. The extinction coefficient was calculated as

$$\varepsilon = -\frac{1}{2L}\ln\frac{F}{F_0} \tag{13}$$

where F and F_0 are the transmitted radiant fluxes in cloud and in clear sky, respectively.

The range of measurement of the extinction meter depends on the length of the optical path L. For longer optical paths the sensitivity threshold is lowered. However, the maximum measured extinction coefficient decreases with an increase in the optical path. For the current installation on the NRC Twin Otter, the maximum measurable extinction coefficient is about 250 km^{-1}. The lower limit was evaluated from the clear-sky drift as ~2 km^{-1} for this probe installation. As a frame of reference, this corresponds to a 10 μm monodisperse cloud droplet concentration and LWC of 13 cm^{-3} and 0.007 gm^{-3}, respectively. For a 100 μm monodisperse spectrum the corresponding concentration and LWC values are 0.13 cm^{-3} and 0.07 gm^{-3}, respectively. On average, the accuracy of the extinction meter is estimated as 12% [*Kosarev et al.*, 1976].

4. Experimental Results

4.1. Comparisons of Extinction Coefficient and LWC

Figure 2a shows a comparison of LWC derived from the FSSP with direct measurements by the King and Nevzorov probes. Figure 2b shows the extinction coefficient derived from the FSSP in comparison with the extinction meter. The

Figure 1. Installation of the Nevzorov extinction meter on the National Research Council (NRC) Twin Otter. The optical unit is mounted at the ceiling inside the fuselage. The reflecting prism is installed in a special housing at the top of the tail. The distance between the optical unit and the reflecting prism is 6 m. The solid line with arrows shows the path of the light beam.

measurements were conducted in warm marine *St-Sc* in horizontal flight at two different altitudes: 600 m (1420-1439 (UT)) and 200 m (1443-1453 (UT)). The droplet size spectra were unimodal in the cloud shown on the left-hand side of Figure 2 with the modal diameter varying from 5 to 8 μm and droplet number concentration about 450 cm^{-3}. The droplet size spectra in the cloud on the right-hand side of Figure 2 were both bimodal and unimodal with the modal diameter varying from 5 to 16 μm with droplet number concentration about 200 cm^{-3}. On the basis of measurements from the OAP-2D Grey in both clouds, there were no droplets larger 50 μm.

Figure 3 shows contoured scatter diagrams of LWC and the extinction coefficient derived from FSSP data and the same parameters measured by the King, Nevzorov, and extinction probes. The isolines show the changes of the parameters between minimum and maximum values with a step of 10%. For a particular case, the LWC measured by the FSSP and that measured by the hot wire probes agrees within 5-6%. The extinction coefficient derived from the FSSP and that measured by the extinction probe agrees within 7%.

Besides good tuning of the probes, another reason for such a good agreement is the absence of droplets outside of the FSSP size range, which in some cases could significantly reduce the calculated values of LWC and extinction.

Since the extinction coefficient and LWC are the second and third moments of the droplet size distribution, there is only one unique combination of FSSP size bin thresholds that can provide ε_{FSSP} and W_{FSSP} values consistent with ε_{Nevz} and W_{King}, respectively, for various droplet size spectra. Note therefore that it is theoretically possible to retrieve the thresholds of FSSP droplet size bins from direct measurements of the extinction coefficient (using a transmissometer), LWC (hot wire probes), and FSSP droplet spectra. In order to solve this inverse problem the chosen droplet size spectra should not have droplets outside the range of FSSP, which can affect ε_{FSSP} and W_{FSSP}. Potentially, this may be a useful method for validating the FSSP size thresholds, since they are derived from comparisons of measurements of three independent probes, using different principles. This kind of validation may be important during long field projects, when the FSSP calibration may change with time because of optic contamination and misalignment.

4.2. Comparisons of D_{eff}

Figure 2c shows a comparison of D_{eff} derived from the FSSP using equation (2), and that calculated from the King and Nevzorov hot wire probes and the extinction meter measurements using equation (5). This comparison demonstrates a relatively good agreement between these two independent methods of calculating D_{eff}. Figure 4a shows a contoured scatter diagram for D_{eff} measured by the different methods for the clouds shown in Figure 2. The effective diameter derived from the two different methods agrees on average within 6%.

4.3. Comparison of N_{eff}

Figure 2d shows the time histories of the FSSP total number concentration, the effective concentration derived from

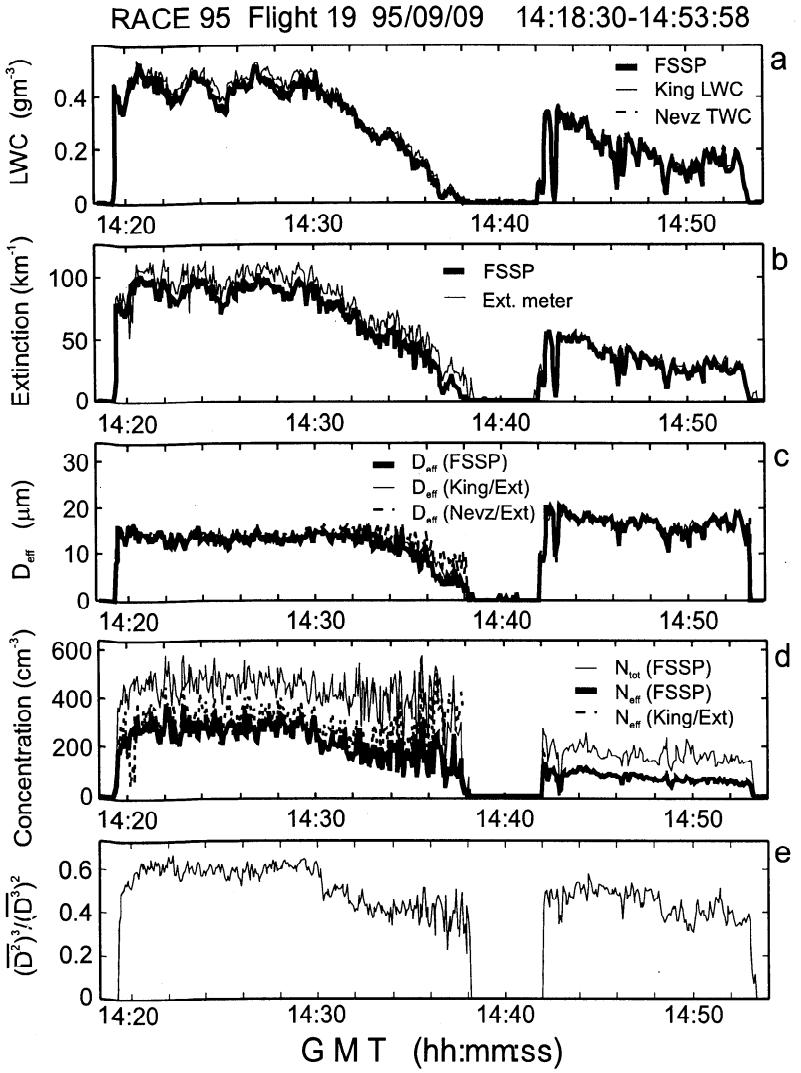

Figure 2. Variations of (a) liquid water content derived from the FSSP and that measured by hot wire King and Nevzorov probes; (b) extinction coefficient measured by the extinction meter and that derived from the FSSP; (c) effective diameter derived from the FSSP (equation (2)) and effective diameters calculated from measurements of LWC (King and Nevzorov probes) and extinction meter (equation (8)); (d) droplet number concentration measured by the FSSP, effective concentration derived from the FSSP (equation (12)), and that calculated from the King probe and extinction meter (equation (11)); and (e) the ratio $\left(\overline{D^2}\right)^3 / \left(\overline{D^3}\right)^2 = N_{eff}/N_0$. Nova Scotia; *St-Sc*; September 9, 1995; T=15°C.

the FSSP (equation (12)) with that calculated from measurements of the King probe, and the extinction meter (equation (11)). Figure 4b shows a contoured scatter diagram for the effective concentration calculated from the two different methods. They agree on average within 14%. The agreement is worse than that for D_{eff} in Figure 4a. The reason for this is that the method of calculation of N_{eff} from equation (11) may give larger errors than for N_{eff} derived from the FSSP, as was mentioned in section 2.3.

The analysis of data from the RACE project showed that the ratio N_{eff}/N_o on average varies from 0.6 to 0.8. However, in some zones the total droplet number concentration N_o may differ from N_{eff} by a factor of 0.1 to 0.5. From equation (12), this difference is defined by the ratio $\left(\overline{D^2}\right)^3 / \left(\overline{D^3}\right)^2$. The variations of the ratio $\left(\overline{D^2}\right)^3 / \left(\overline{D^3}\right)^2$ are shown in Figure 2e. Measurements in stratiform clouds during the RACE project showed that the ratio $\left(\overline{D^2}\right)^3 / \left(\overline{D^3}\right)^2$ has a tendency to stay constant on horizontal legs. However, it may strongly vary with altitude. Figure 5 shows the time histories of the aircraft altitude, LWC, extinction, D_{eff}, N_0, N_{eff}, and the ratio $\left(\overline{D^2}\right)^3 / \left(\overline{D^3}\right)^2$ during the descent and ascent in a 400 m deep stratiform cloud. Figures 5b, 5c, 5d and 5e show relatively good agreement among LWC, extinction, D_{eff}, N_{eff} calculated from the FSSP and that derived from the extinction meter, and the hot wire probes. Figure 5f indicates that

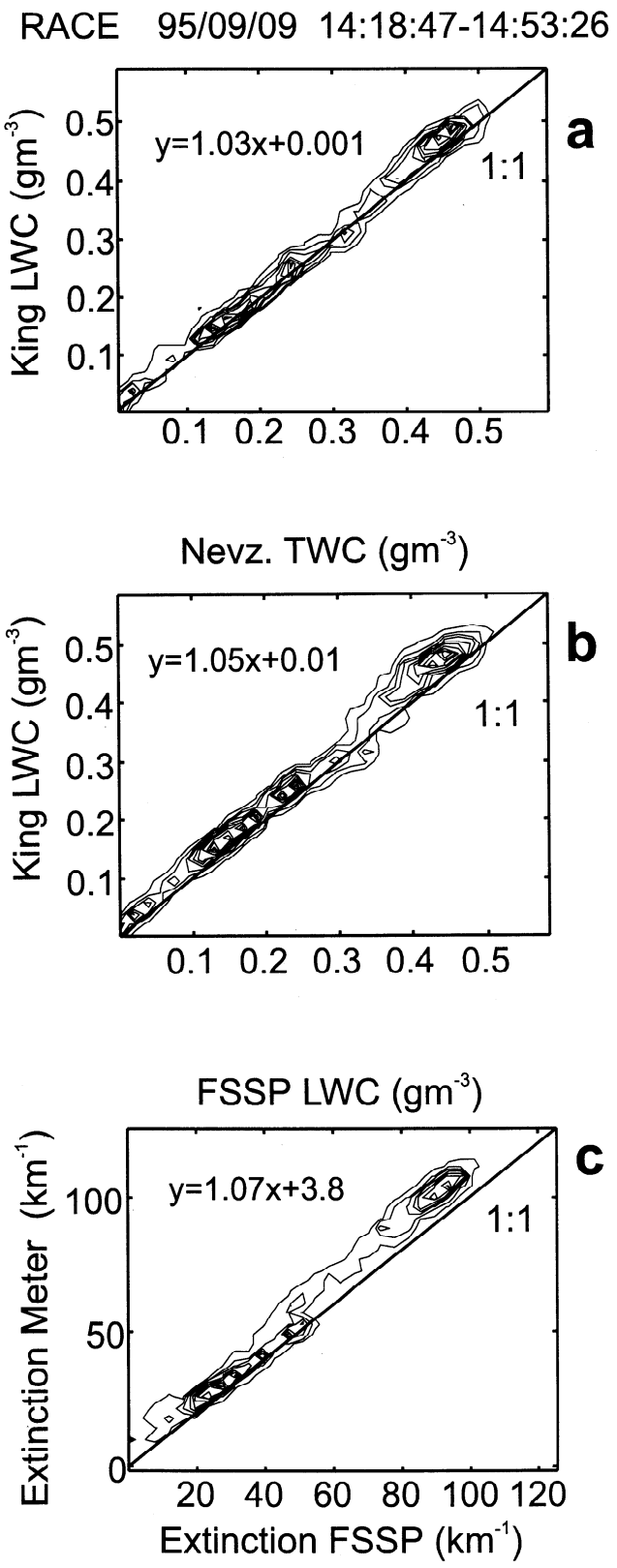

Figure 3. Scatter contour diagrams of (a) LWC measured by the King and Nevzorov probes, (b) LWC derived from the FSSP and that measured by the King probe, (c) extinction coefficient measured by the extinction meter and that derived from the FSSP. The contour diagrams show the isolines of the measured parameter between minimum and maximum values with a step of 10%.

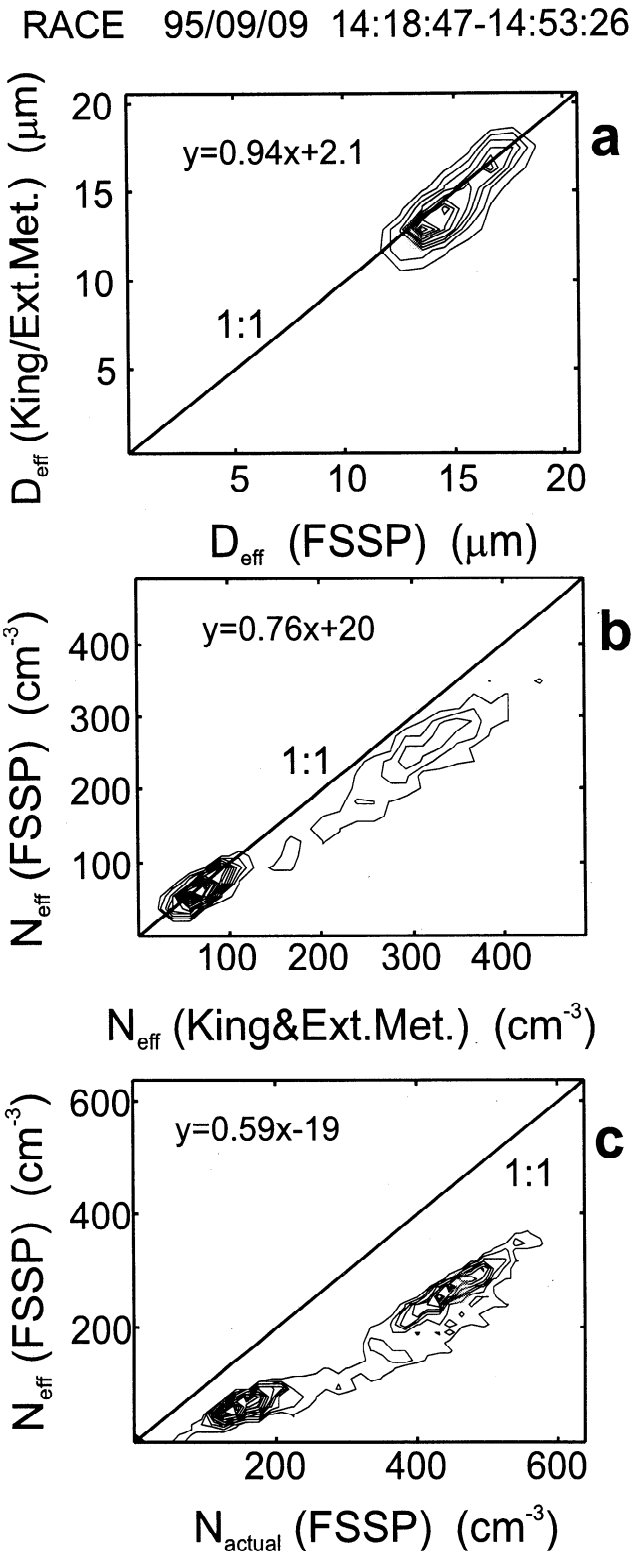

Figure 4. Scatter contour diagrams of (a) effective diameter derived from the FSSP (equation (2)) and calculated from measurements of the King probe and the extinction meter (equation (8)), (b) effective concentration derived from the FSSP (equation (12)); and that calculated from the King probe and extinction meter (equation (11)), (c) droplet number concentration and effective concentration measured by the FSSP. The contour diagrams show the isolines of the measured parameter between minimum and maximum values with a step of 10% (a) and 5% (b, c).

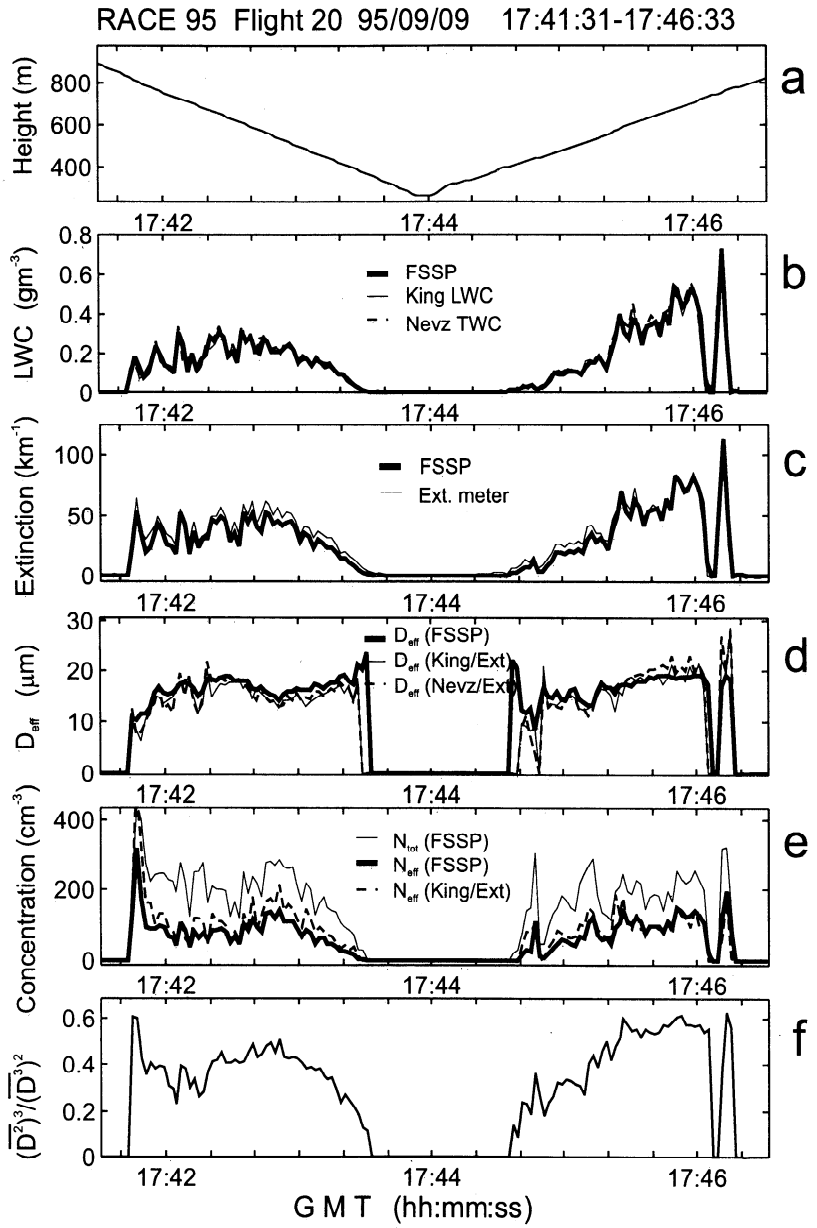

Figure 5. Variations of (a) aircraft altitude; (b) LWC derived from the FSSP and that measured by the hot wire King and Nevzorov probes; (c) extinction coefficient measured by the extinction meter and that derived from the FSSP; (d) effective diameter derived from the FSSP (equation (2)) and effective diameter calculated from measurements of the King, Nevzorov probes and the extinction meter (equation (8)); (e) droplet number concentration measured by the FSSP, effective concentration derived from the FSSP (equation (12)) and that calculated from the King probe and the extinction meter (equation (11)); and (f) the ratio $\left(\overline{D^2}\right)^3 \Big/ \left(\overline{D^3}\right)^2 = N_{eff}/N_0$. Nova Scotia; *St-Sc* ; September 9, 1995; T=14°C – 17°C.

$\left(\overline{D^2}\right)^3 \Big/ \left(\overline{D^3}\right)^2$ increases from 0.1 to 0.6 from the cloud base to the cloud top. This fact is important for parameterization in GCM and numerical weather models.

4.4. Measurements of D_{eff} in Ice Clouds

At present, measurements of the microphysical parameters of ice and mixed phase clouds are a challenge. There are currently no aircraft instruments providing reliable measurements of the ice particle size distribution for the full range of interest. The large variety of ice particle shapes makes the solution of this problem difficult and perhaps impossible using light-scattering techniques (FSSP, Gerber probe, etc.). The imaging technique requires at least 10 to 12 image pixels in order to determine ice particle habit [*Korolev et al.*, 1998a]. Conventional aircraft particle-imaging instruments suffer from a lack of resolution. For example, a PMS OAP-2DC with a 25 μm resolution can distinguish spherical particles from non-spherical only for sizes larger than ~250 μm.

Furthermore, the derivation of mass concentration and extinction coefficient is still a problem even for particles > 250 μm, since the third dimension of the particle and particle density are unknown. In this regard, the direct measurements of total water content and extinction coefficient provided by the Nevzorov LWC/TWC probe and the extinction meter provide a unique capability to measure the extinction, effective diameter, and effective concentration within ice and mixed phase clouds. The measurements of these probes do not require any additional knowledge of the particle phase, shape, density, and orientation of cloud particles.

Figure 6 illustrates the variation of W, ε, D_{eff}, and N_{eff} measured in *Ci nebulosus* at an altitude of 7900 m and a temperature of -46°C. The measurements were made over the European part of Russia using the Nevzorov hot wire TWC probe and extinction meter installed on the Ilushin-18 of the Central Aerological Observatory (Moscow). The extinction meter on the Ilushin-18 had an optical path of L=16 m and therefore provided better sensitivity than the similar Twin Otter measurements. It is seen that in the left-hand section of Figure 6 the effective diameter is almost constant and varies between 5 and 8 μm. In the right-hand section, D_{eff} increases, reaching 50 to 100 μm in some regions. This example demonstrates the possibilities of the suggested method in measurements of D_{eff} and N_{eff} in ice clouds.

5. Discussion

Section 2.2 gives a simple interpretation of N_{eff}: it is a droplet number concentration of a monodisperse size distribution that has the same W, ε, and D_{eff} as the droplet size distribution $f(D)$. The effective concentration may potentially play an important role in future parameterization of clouds, since four parameters of droplet size distribution W, ε, D_{eff}, and N_{eff} form a closed system of parameters (i.e., any two parameters define the system and thus the other two parameters). In simple terms, an arbitrary droplet size distribution is replaced by a monodisperse size spectrum with the same W, ε, and D_{eff}. The four variables W, ε, D_{eff}, and N_{eff} may form a system of parameters well suited for modeling cloud radiative processes. The introduction of the effective concentration allows for model calculations of the effect of droplet number concentration while maintaining a self-consistent system of variables.

Some researchers assume for the parameterization of cloud microstructure that

$$D_{eff} = \left(\frac{6W}{\pi \rho K N_0} \right)^{1/3} \tag{14}$$

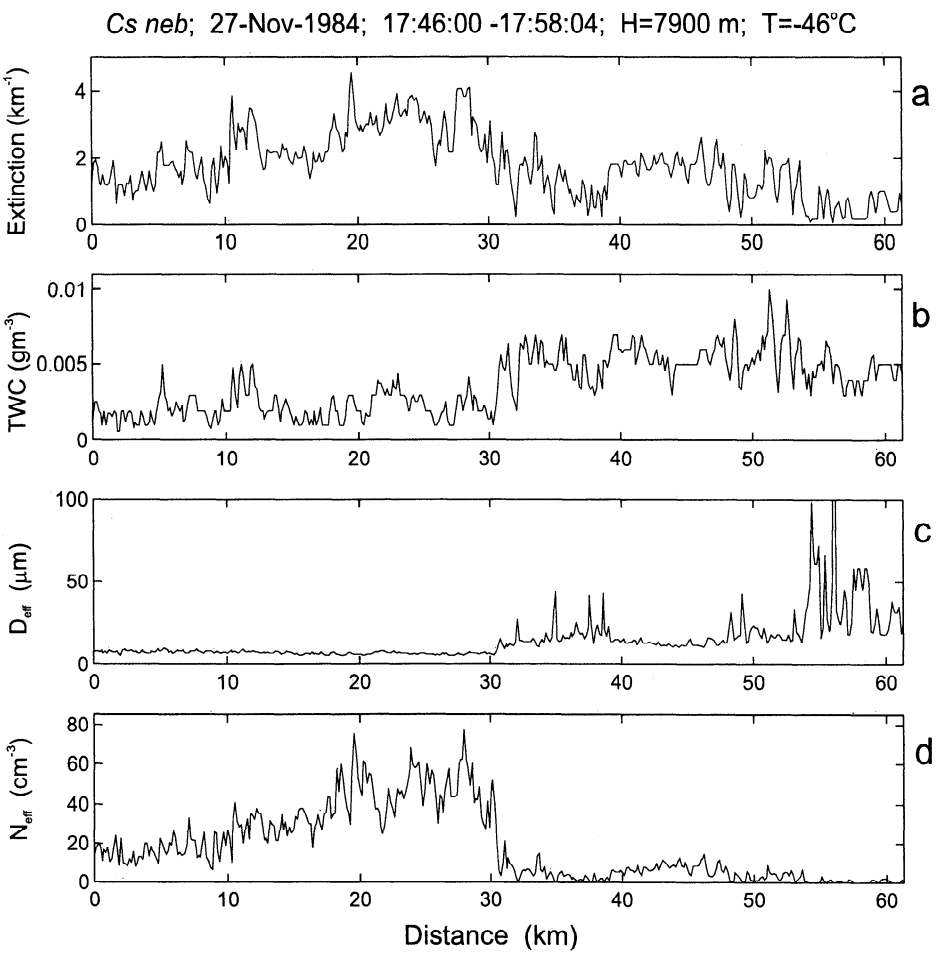

Figure 6. Variations of (a) extinction coefficient measured by the extinction meter; (b) total water content measured by the Nevzorov TWC probe; (c) effective diameter; and (d) effective concentration in *Cs nebulosus*, H = 7900 m, T = -46°C. The measurements were made from an Ilushin-18 over the European part of Russia on November 27, 1984, 194600-195804 (UT).

where K is a coefficient that varies between 0.6 and 1 [e.g., *Fouquart et al.*, 1990; *Bower and Choularton*, 1992]. *Martin et al.* [1994] found that $K = \overline{D^3} / D_{eff}^3$.

In fact, equations (9) and (12) yield

$$D_{eff} = \left(\frac{6W}{\pi \rho N_{eff}} \right)^{1/3} \tag{15}$$

where $N_{eff}=KN_0$; and from equation (12), the coefficient K can be represented by one of the three following ways:

$$K = \frac{\left(\overline{D^2}\right)^3}{\left(\overline{D^3}\right)^2} = \frac{\overline{D^2}}{D_{eff}^2} = \frac{\overline{D^3}}{D_{eff}^3}. \tag{16}$$

Since for any droplet size distribution $D_{eff} \geq \sqrt[3]{\overline{D^3}} \geq \sqrt[2]{\overline{D^2}}$, then $K \leq 1$ for all conditions. The equality $K=1$ is achieved only for a monodisperse size distribution, then from equation (12) $N_0=N_{eff}$. The difference between N_0 and N_{eff} reflects the shape of droplet size distribution. The narrower the droplet size distribution, the less is the difference between N_0 and N_{eff}, and the coefficient K is closer to unity.

The measurements in stratiform clouds averaged over 1 s intervals (~ 80 m) made during the RACE project, showed that the coefficient K may vary from 0.1 to 0.95. Average values change from cloud to cloud and it can vary from about 0.6 to 0.8. This is consistent with the study of *Martin et al.* [1994], though during the RACE project, there was no distinct difference in K for marine and continental stratiform clouds. It should be noted that the coefficient K strongly varies in a cloud layer with height. On average, it increases from cloud base to the cloud top (Figure 5). For the further parameterization of cloud microstructure in a GCM and numerical weather prediction models, this fact should be taken into account.

6. Conclusions

A new method for measuring extinction and D_{eff} in clouds, using a hot wire device and transmissometer, has been demonstrated. In liquid or mixed phase clouds, transmission (and thereby extinction) is measured directly with relatively small errors. These estimates are not subject to the formidable errors inherent in integrating size distributions derived from particle spectrometers, especially in the case of ice particles. This in itself is an important contribution to the improvement of the measurement of radiative properties of clouds. In liquid-only clouds, a straightforward calculation of D_{eff} from extinction and hot wire LWC measurements provides an estimate free of the limitations of truncated size ranges and poor overlap present in current estimates from PMS FSSP and OAP probes. The method was shown to give very comparable results to measurements from PMS probes in situations favorable to the latter. In ice or mixed phase clouds the D_{eff} calculation is not subject to a number of the problems associated with such calculations from conventional spectrometers, such as the uncertainty in particle sizing and phase discrimination for particles smaller than ~100 μm, the uncertainties in sizing and concentration in probe overlap regions, and interpretation of particle diameter from a two-dimensional particle image. The proposed method provides a value of D_{eff} in ice or mixed phase clouds, which is consistent with one of the basic radiative properties of the cloud (transmission) and one of the basic cloud bulk parameters (ice water plus liquid water content). In spite of these possible advantages, further work is required to compare the ice or mixed phase cloud estimates of D_{eff} from this method to conventional methods with cloud spectrometer and in the end, the use of a combination of microphysical probes may prove to be the most prudent measurement strategy.

A newly introduced parameter, the effective number concentration, may provide a convenient model variable for assessing the effects of droplet number concentration in a self-consistent system of four cloud particle spectrum variables. This parameter may also provide an independent measurement for the evaluation of the actual particle number concentration in cloud.

Acknowledgements. The authors wish to thank the Institute for Aerospace Research of the National Research Council (NRC) for their participation in RACE, led by Dave Marcotte. Special appreciation also goes to Cathy Banic and W. Richard Leaitch of AES, who directed most of the Twin Otter flights, and technical support provided by Mohammed Wasey and Steve Bacic of AES. We also appreciate the discussion and comments of Ilia Mazin of CAO and Howard Barker and W. Richard Leaitch of AES.

References

Baumgardner, D., and A. V. Korolev, Airspeed corrections for Optical Array Probe sample volume, *J. Atmos. Oceanic Technol.*, *14*, 1224-1229, 1997.

Baumgardner, D., and M. Spowart, Evaluation of the Forward Scattering Spectrometer Probe, III, Time response and laser inhomogeneity limitations, *J. Atmos. Oceanic Technol.*, *7*, 666-672, 1990.

Baumgardner, D., J. W. Strapp, and J. E. Dye, Evaluation of Forward Scattering Spectrometer Probe, II, Correction for coincidence and dead-time losses, *J. Atmos. Oceanic Technol.*, *2*, 626-632, 1985.

Biter, C. J., J. E. Dye, D. Huffman, and W. D. King, The drop response of the CSIRO liquid water content, *J. Atmos. Oceanic Technol.*, *4*, 359-367, 1987.

Bower, K. N., and T. W. Choularton, A parameterization of the effective radius of ice free clouds for use in global climate models, *Atmos. Res.*, *27*, 305-339, 1992.

Brenguier, J. L., Coincidence and dead time corrections for particle counters. Part II: High concentration measurements with FSSP, *J. Atmos. Oceanic Technol.*, *6*, 585-598, 1989.

Charlson, R. J., J. E. Lovelock, M. O. Andreae, and S. G. Warren, Ocean phytoplankton, atmospheric sulphur, cloud albedo and climate, *Nature*, *326*, 655-661, 1987.

Dadlin, P., C. Pontikis, and E. Hicks, Sensitivity of a GCM to changes in the droplet effective radius parameterisation, *Geophys. Res. Lett.*, *24*, 437-440, 1997.

Ebert, E. E., and J. A. Curry, A parameterization of ice cloud optical properties for climate models, *J. Geophys. Res.*, *97*, 3831-3836, 1992.

Foot, J. S., Some observations of the optical properties of clouds, II Cirrus, *Q. J. R. Meteorol. Soc.*, *114*, 145-164, 1988.

Fouquart, Y., J. C. Buries, M. Herman, and R. S. Kandel, The influence of clouds on radiation: A climate-modelling perspective, *Rev. Geophys.*, *28*, 145-166, 1990.

Gardiner, B. A., and J. Hallet, Degradation of in-cloud Forward Scattering Spectrometer Probe measurements in the presence of ice particles, *J. Atmos. Oceanic Technol.*, *2*, 171-180, 1985.

Gayet, J. F., G. Febvre, and H. Larsen, The reliability of the PMS FSSP in the presence of small ice crystals, *J. Atmos. Oceanic Technol.*, *13*, 1300-1310, 1996.

Hansen, J. E., and L. D. Travis, Light scattering in planetary atmospheres, *Space Sci. Rev.*, *16*, 527-610, 1974.

Heymsfield, A. J., and C. M. R. Platt, A parameterisation of the particle size spectrum of ice clouds in terms of the ambient temperature and ice water content, *J. Atmos. Sci.*, *41*, 846-855, 1984.

King, W. D., and R. J. Handsworth, Total droplet concentration and average droplet sizes from simultaneous liquid water content and extinction measurements, *J. Appl. Meteorol.*, *18*, 940-944, 1979.

King, W. D., D. A. Parkin, and R. J. Handsworth, A hot wire water device having fully calculable response characteristics, *J. Appl. Meteorol.*, *17*, 1809-1813, 1978.

Knollenberg, R. G., Techniques for probing cloud microstructure, in *Clouds, Their Formation, Optical Properties, and Effects*, edited by P. V Hobbs, and A. Deepak, 495 pp., Academic, San Diego, Calif., 1981.

Korolev, A. V., J. W. Strapp, and G. A. Isaac, On the accuracy of PMS Optical Array Probes, *J. Atmos. Oceanic Technol.*, *15*, 708-720, 1998a.

Korolev, A. V., J. W. Strapp, G. A. Isaac, and A. N. Nevzorov, The Nevzorov airborne hot wire LWC/TWC probe: Principal of operation and performance characteristics, *J. Atmos. Oceanic Technol.*, *15*, 1495-1510, 1998b.

Kosarev, A. L., I. P. Mazin, A. N. Nevzorov, and V. F. Shugaev, Optical density of clouds (in Russian), *Trans. Cent. Aerol. Obs.*, *124*, 10-43, 1976.

Martin, C. M, D. W. Johnson, and A. Spice, The measurements and parameterisation of effective radius of droplets in warm stratocumulus clouds, *J. Atmos. Sci.*, *51*, 1823-1842, 1994.

Mazin, I. P., N. A. Monakhova, and V. F. Shugaev, Vertical distribution of water content and optical characteristics of continental stratiform clouds, *Russ. Meteorol. Hydrol.*, *9*, 9-29, 1996.

Mitchel, J. F., C. A. Senior, and W. J. Ingram, CO_2 and climate: A missing feedback?, *Nature*, *341*, 132-134, 1989.

Nevzorov, A. N., Aircraft cloud water content meter, *in Communications à la 8ème Conférence Internationale sur la Physique des Nuages,* vol. II, pp. 701-703, Clermont-Ferrand, France, 1980.

Nevzorov A. N., and V. F. Shugaev, The use of integral parameters for study of cloud microstructure (in Russian), *Trans. Cent. Aerol. Obs.*, *101*, 32-47, 1972.

Nevzorov A. N., and V. F. Shugaev, Aircraft cloud extinction meter(in Russian), *Trans. of Cent. Aerol. Obs.*, *106*, 3-10, 1974.

Platt, C. M. R., and Harshvardhan, Temperature dependence of cirrus extinction: implication for climate feedback, *J. Geophys. Res.*, *20*, 11051-11058, 1988.

Slingo, A., Sensitivity of the earth's radiation budget to changes in low clouds, *Nature*, *343*, 49-51, 1990.

Slingo, A., and H. M. Schencker, On the shortwave radiative properties of stratiform water clouds, *Q. J. R. Meteorol. Soc.*, *108*, 407-426, 1982.

Stephens, G. L., Radiation profiles in extended water clouds, II, Parameterization scheme, *J. Atmos. Sci.*, *35*, 2123-2132, 1978.

Stephens, G. L., and P. L. Webster, Clouds and climate: Sensitivity to simple systems, *J. Atmos. Sci.*, *38*, 235-247, 1981.

Twomey, S., The influence of pollution of the shortwave radiation of clouds, *J. Atmos. Sci.*, *34*, 1149-1152, 1977.

van de Hulst, H. C., *Light Scattering by Small Particles*, 470 pp., John Wiley, New York, 1957.

Wendisch, M., A. Keil, and A. V. Korolev, FSSP characterisation with monodisperse water droplets, *J. Atmos. Oceanic Technol.*, *13*, 1152-1165, 1996.

G.A. Isaac, A.V. Korolev, and J. W. Strapp, Atmospheric Environment Service, Cloud Physics Research Division, 4905 Dufferin Street, Downsview, Ontario, Canada M3H 5T4 (Email: george.isaac@ec.gc.ca; akorolev@rpn.aes.doe.ca; walter.strapp@ec.gc.ca)

A.N. Nevzorov, Central Aerological Observatory, Pervomayskaya St. 3, Moscow, 141700, Russia

(Received June 24, 1998; revised September 15, 1998; accepted October 13, 1998.)